Interleukin-7 co-ordinates proliferation, differentiation and *Tcra* recombination during thymocyte β-selection

Amine Boudil[1,2], **Irina R. Matei**[1], **Han-Yu Shih**[3], **Goce Bogdanoski**[1], **Julie S. Yuan**[1], **Stephen G. Chang**[1], **Bertrand Montpellier**[1,2], **Paul E. Kowalski**[1], **Veronique Voisin**[4], **Shaheena Bashir**[4], **Gary D. Bader**[4,5], **Michael S. Krangel**[3], and **Cynthia J. Guidos**[1,2,*]

[1]Program in Developmental and Stem Cell Biology, Hospital for Sick Children Research Institute, Toronto, ON, Canada

[2]Department of Immunology, University of Toronto, Toronto, ON, Canada

[3]Department of Immunology, Duke University Medical Center, Durham, NC, USA

[4]The Donnelly Centre, University of Toronto, ON, Canada

[5]Department of Molecular Genetics, University of Toronto, Toronto, ON, Canada

Abstract

pre-T cell receptor (TCR) and Notch signaling induce transient self-renewal or "β-selection" of TCRβ+ CD4 CD8 double-negative-3 (DN3) and DN4 progenitors that differentiate into CD4 CD8 double positive (DP) thymocytes which then rearrange *Tcra*. Interleukin-7 (IL-7) promotes Bcl2-dependent survival of TCRβ− DN thymocytes, but IL-7 functions during β-selection remain unclear. Here, we show that IL-7 signals TCRβ+ DN3 and DN4 thymocytes to upregulate genes involved in cell growth and represses *Bcl6*. Accordingly, IL-7-deficient DN4 cells lacked trophic receptors and did not proliferate, but rearranged *Tcra* prematurely and differentiated rapidly. *Bcl6* deletion, but not *BCL2* over-expression, partially restored DN4 self-renewal in the absence of IL-7. Thus, IL-7 critically collaborates with pre-TCR and Notch signaling to coordinate proliferation, differentiation and *Tcra* recombination during β-selection.

INTRODUCTION

During intrathymic T cell development, Notch1 signaling maintains survival and promotes T lineage commitment as CD44+ CD25− DN1 cells differentiate into CD44+ CD25+ DN2 and

*Corresponding author: Cynthia J. Guidos, Peter Gilgan Centre for Research and Learning, 686 Bay Street, Toronto, ON, Canada M5G 0A4; cynthia.guidos@sickkids.ca; PH: (416) 813-5026.

Author Contributions
A.B., I.R.M., B.M., H-Y.S., G.B., S.G.C., J.S.Y., P.E.K. designed, performed and analyzed experiments. V.V., S.B. and G.D.B. performed statistical analysis and GSEA of Illumina gene expression data; A.B., H-Y.S. and M.S.K. wrote the manuscript. C.J.G. analyzed data, supervised the study and wrote the manuscript.

Competing Interests Statement
The authors declare no competing financial interests.

CD44^{lo} CD25$^+$ DN3a cells[1]. Mice lacking the *interleukin-7* (*Il7*) or *Il7 receptor* (*Il7r*) genes have very few DN2 and DN3 cells, in part because they depend on IL-7 signaling to induce expression of *Bcl2*, a pro-survival gene[2]. Indeed, transgenic expression of human *BCL2* (*BCL2*)[3, 4] or deletion of *Bax* or *Bim* pro-apoptotic genes[5, 6] significantly restores both DN2-DN3 and mature single positive (SP) compartments in *Il7r*$^{-/-}$ or γc$^{-/-}$ mice. Thus, IL-7 induces Bcl2-mediated survival of T-lineage committed DN2-DN3a progenitors as they become quiescent and rearrange T cell receptor (*Tcr*) *gamma, delta* and *beta* (*Tcrg, Tcrd* and *Tcrb*) gene segments. Subsequent proliferation and differentiation of αβ T cell progenitors requires successful *Tcrb* rearrangement and expression of intracellular TCRβ (icTCRβ) protein to form the pre-TCR signaling complex and initiate "β-selection". Although IL7R expression persists through the early stages of β-selection, the importance of IL-7 signaling in this process has not been resolved.

pre-TCR and Notch1 signaling co-operate to initiate β-selection[7] by inducing quiescent DN3a cells to down-regulate expression of *Recombination activating genes* (*Rag*) and become large cycling DN3b cells that up-regulate transferrin receptor (Tfrc or CD71) and other trophic receptors[8]. These pre-TCR and Notch1-induced changes promote rapid self-renewal of DN3b cells as they lose CD25 and differentiate sequentially into cycling DN4, CD8 immature single positive (ISP) and early DP (eDP) blast cells, which then cease proliferating and become quiescent late DP (lDP) cells. However, it is unclear whether pre-TCR and Notch1 signaling are sufficient to maintain trophic responses, proliferation and differentiation during β-selection *in vivo*.

Rag expression declines precipitously after the DN3a stage, so efficient *Tcra* rearrangement requires *Rag* re-expression in DP thymocytes[9]. *Tcra* recombination normally initiates in eDP cells using the most 3' Vα and 5' Jα gene segments. If DP thymocytes fail to be positively selected after primary *Tcra* rearrangement, secondary rearrangements that use progressively more distal 5' Vα and 3' Jα gene segments occur, but only in non-cycling lDP cells[10]. The *Tcra-Eα* enhancer, located 3' of the *Jα* array, modifies *Tcra* locus chromatin to make 3' Vα segments and 5'Jα gene segments accessible to Rag, facilitating their synapsis and recombination[11]. Although *Tcra* rearrangement is restricted to DP thymocytes, Eα may be activated as early as the DN4 stage by transcription factors induced by pre-TCR signaling[12]. During the pre-B cell receptor (pre-BCR) induced pro-B to pre-B transition, IL-7 induces proliferation and represses *Ig kappa* rearrangement by a STAT5-dependent epigenetic mechanism[13, 14]. STAT5 also represses *Bcl6* expression to prevent p53-induced apoptosis during *Ig* light chain recombination in pre-B cells[15, 16]. *Bcl6* is best known as a transcriptional repressor with critical functions in germinal center responses and as a potent B cell oncogene[17]. Interestingly, thymocytes strongly up-regulate *Bcl6* as proliferation ceases during the DN3-DP transition (www.Immgen.org), but the regulation and functions of *Bcl6* during T cell development have not been defined.

There are conflicting reports on the role of IL-7 signaling in β-selection. IL7R expression is not lost until the ISP stage[18], but DN4 thymocytes were reported to be unresponsive to IL-7[19]. Studies using antibodies to block IL-7 signaling *in vitro* concluded that IL-7 signaling is dispensable for β-selection of DN3 cells[20]. In contrast, another group reported, using a similar approach, that IL-7 signaling is required for DN4 survival but not

proliferation[21]. Yet other studies in which IL-7 signaling was artificially augmented *in vitro* concluded that IL-7 signaling actively inhibits β-selection, in part by impairing expression of *Tcf7* (encoding TCF1), *Lef1* and *Rorc*[18]. Therefore, *in vitro* studies have reached conflicting conclusions on the importance of IL-7 signaling during β-selection.

Here, we report that early post-β-selection DN3b and DN4 thymocytes respond to IL-7 *in vitro* and *in vivo*. IL-7 signaling acutely induces many genes involved in protein translation, cell growth and metabolism, and also represses *Bcl6*. Accordingly, we showed that IL-7 is required *in vivo* for robust clonal expansion, to enforce the canonical DN3b–DN4-ISP-DP differentiation sequence, and to prevent premature *Tcra* rearrangement in DN thymocytes. Thus, we identified a novel role for IL-7 signaling during β-selection that includes repression of *Bcl6* to allow self-renewal of DN4 cells. In contrast to IL-7 functions at earlier and later stages of T cell development, the functions of IL-7 during β-selection cannot be replaced by *BCL2*.

RESULTS

IL-7 signaling in post-β-selection DN thymocytes

We first compared IL7R expression and function in pre- versus post-β-selection DN thymocytes. In contrast to prior studies, we used icTCRβ to positively identify β-selected cells within the heterogeneous DN3 and DN4 subsets (Supplementary Fig. 1)[19]. As expected, pre-selection icTCRβ⁻ DN3a cells were IL7R^hi and robustly phosphorylated STAT5 after IL-7 stimulation *in vitro* (Fig. 1a). Post-selection DN3b and DN4 cells also expressed IL7R and IL-7 stimulation induced pSTAT5. Normalized amounts of IL7R and IL-7-induced STAT5 phosphorylation were highest in DN3b and lowest in DN4 cells. Nonetheless, IL-7 stimulation increased survival of DN3a, DN3b and DN4 cells to similar extents (Fig. 1a). Thus, pre-selection DN3a and post-selection DN3b–DN4 thymocytes were similarly responsive to IL-7-mediated survival signaling *in vitro*. Importantly, fresh *ex vivo* DN3b and DN4 *Il7r*^{+/+} wild-type (WT) thymocytes expressed considerably higher amounts of pSTAT5 and murine Bcl2 (mBcl2) than those from *Il7r*^{−/−} mice (Fig. 1b), indicating that they respond to physiological levels of IL-7 produced intrathymically.

To determine if human *BCL2* can restore both pre- and post-β-selection compartments in IL-7-deficient mice, we generated transgenic *Il7r*^{−/−} mice expressing *BCL2* under control of the *Lck*-proximal promoter. Accordingly, hBcl-2 was expressed in some DN2 cells and in all downstream cells (Fig. 2a). Although hBcl-2 increased DN3a cell numbers 30-fold in *Il7r*^{−/−} mice, it did not increase cellularity of the DN3b, DN4 or DP compartments (Fig. 2b). However, hBcl-2 significantly restored CD4 and CD8 SP thymocyte cellularity, 7- and 10-fold, respectively. These findings identify an important function for IL-7 signaling during β-selection *in vivo* that, in contrast to earlier and later stages of T cell development, cannot be replaced by *BCL2*.

Transcriptional responses to IL-7

The failure of *BCL2* to restore post-β-selection DN or DP thymocyte compartments in *Il7r*^{−/−} mice suggested that IL-7 activates other pathways critical for β-selection *in vivo*.

Therefore, we used Illumina gene expression profiling to globally identify pathways acutely regulated by IL-7 in DN3a, DN3b and DN4 cells. Importantly, all 3 subsets showed robust induction of direct Jak-STAT target genes after 3h of IL-7 stimulation (Fig. 3a). This group included *Bcl2* and *Cish, Socs2* and *Socs3*, feedback regulators of Jak-STAT signaling, as well as *Pim1, Tfrc* (*Cd71)* and *Ccnd2*. Thus, in addition to inducing survival genes, IL-7 acutely regulates expression of trophic receptors and cell cycle regulators in pre- and post-β-selection DN thymocytes.

The response to IL-7 stimulation was robust and complex in all 3 subsets, although the number of transcripts significantly altered by IL-7 declined substantially as DN3a cells matured into DN3b and DN4 cells (Supplementary Fig. 2a). Il-7 stimulation acutely altered expression of large numbers of genes involved in signaling, translation, metabolism and cell growth (Supplementary Fig. 2b, c; Supplementary Table 1, 2). The most potently induced nutrient transporter was *Slc7a5* (Supplementary Fig. 2c), which encodes a large neutral amino acid transporter required for metabolic reprogramming during T cell activation and effector differentiation[22]. The signaling group included several genes encoding GTP binding proteins, Ras-MAPK and PI3K–mTOR proteins as well as signaling receptors (Fig. 3b). Finally, IL-7 increased expression of transcriptional regulators, most notably *Bhlhe40* (Fig. 3b), whose importance in T cell development is unknown. Although the magnitude and significance of IL-7-induced transcriptional changes were generally more robust in pre-selection DN3a cells, some genes in each category were more highly induced in post-β-selection DN cells (starred in Fig. 3), suggesting co-operative regulation with pre-TCR signaling.

IL-7 promotes DN4 cell growth and proliferation

Since IL-7 significantly increased expression of many genes that regulate metabolism, signaling and growth, we evaluated the impact of IL-7 deficiency on cell size, a reflection of cellular metabolism and proliferation during β-selection. Although the size of DN3b cells from *Il7r*$^{+/+}$ vs *Il7r*$^{-/-}$ mice was similar, *Il7r*$^{-/-}$ DN4 cells were much smaller than their WT counterparts, suggesting loss of trophic signaling (Fig. 4a). Furthermore, IL-7 deficiency significantly impaired BrDU uptake by *Il7r*$^{-/-}$ DN4 cells, but not DN3b cells (Fig. 4b). *BCL2* over-expression did not prevent atrophy or restore proliferation of *Il7r*$^{-/-}$ DN4 cells, strongly suggesting that IL-7 signaling is required to maintain DN4 thymocyte trophic responses and proliferation *in vivo*, rather than simply to maintain Bcl2-dependent survival.

DN3b and DN4 cells self-renew extensively in a pre-TCR-dependent fashion when cultured with OP9 stromal cells expressing Delta-like Notch ligands and IL-7, and up-regulation of trophic receptors such as CD71 and CD98 (neutral amino acid transporter) shows Notch-dependence in these assays[8, 23]. Because Notch signaling can regulate IL7R expression in some contexts[24, 25], Notch effects on trophic receptors could be IL-7-mediated. We therefore assessed the requirement for IL-7 signaling for inducing CD71 and CD98 during β-selection *in vivo*. As expected, WT DN3b and DN4 cells were CD71^{hi} CD98^{hi} (Fig. 4c). In striking contrast, *Il7r*$^{-/-}$ DN4 cells lacked these trophic receptors, as well as CD27, CD28 and CD24 (data not shown), although DN3b cells expressed normal amounts of these markers. Once again, hBcl-2 did not restore CD71 and CD98 expression to *Il7r*$^{-/-}$ DN4

cells. Although IL-7 increased CD71 expression in stromal-cell free cultures, it did not stimulate DN4 cell proliferation (Fig. 4d), demonstrating that IL-7 signaling cannot promote DN4 self-renewal without Notch activation. Furthermore, Notch-induced proliferation of DN4 cells is IL-7-dependent (Fig. 4e). Collectively, these experiments demonstrate that IL-7 signaling maintains DN4 nutrient receptor expression, and that Notch and IL-7 co-operate to promote self-renewal of DN4 cells.

IL-7 enforces the canonical DN3b–DN4-ISP sequence

DN4 cells are also referred to as "pre-DP" cells because they rapidly generate DP progeny when cultured without stroma or cytokines[26]. Therefore, we evaluated the differentiation potential and kinetics of WT versus $Il7^{-/-}$ DN3b and DN4 cells in stromal cell-free cultures with and without exogenous IL-7. Surprisingly, $Il7^{-/-}$ DN3b cells generated significantly more DP progeny than WT DN3b cells after 15h of culture without IL-7 (Fig. 5a). However, both DN and ISP progeny of $Il7^{-/-}$ DN3b cells retained CD25 expression (Supplementary Fig. 3a), suggesting that mutant DN3b cells generated ISP cells without obviously passing through the CD25− DN4 stage. $Il7^{-/-}$ DN4 cells also generated significantly more DP progeny than WT DN4 cells after 15h, demonstrating that they have enhanced "pre-DP" capacity (Fig. 5b). Strikingly, most $Il7^{-/-}$ DN4 cells became DP within 5h and appeared not to pass through the ISP stage, whereas WT DN4 cells generated only ISP intermediates during this time (Fig. 5c). IL-7 addition to DN3b cells also increased ISP frequency at the expense of DP cell generation, but this impact of IL-7 was significant only for $Il7^{-/-}$ DN3b cells (Supplementary Fig. 3b). IL-7 also increased ISP frequency in cultures of WT but not $Il7^{-/-}$ DN4 progenitors, (Fig. 5b, Supplementary Fig. 3b), indicating that $Il7^{-/-}$ DN4 cells, in contrast to WT DN4 cells, are insensitive to IL-7. Collectively, these experiments suggest that $Il7^{-/-}$ DN3b cells generate ISP and DP progeny without obviously passing through the DN4 stage, whereas $Il7^{-/-}$ DN4 cells rapidly generate DP progeny without obviously passing through the ISP stage.

Bcl6 deletion improves DN4 self-renewal

We noted that *Bcl6* was the most significantly down-regulated gene after IL-7 treatment of DN3a, DN3b and DN4 cells, with FDR-adjusted q-values of 10^{-18}, $4.2×10^{-20}$ and $2×10^{-12}$, respectively (Fig. 6a, Supplementary Table 2). Furthermore, DN3b and DN4 cells from $Il7^{-/-}$ mice expressed significantly more *Bcl6* mRNA than their WT counterparts, suggesting loss of IL-7-mediated repression. Interestingly, normal thymocytes strongly up-regulate *Bcl6* expression as proliferation ceases during the DN3-DP transition (www.Immgen.org), but its functions in T cell development have not yet been identified. Therefore, we asked whether IL-7-induced repression of *Bcl6* in DN4 cells is important for differentiation and self-renewal during β-selection. Because $Bcl6^{-/-}$ mice develop a lethal inflammatory disease[27, 28], we generated DN4 thymocytes by co-culturing WT or $Bcl6^{-/-}$ fetal liver hematopoietic progenitor cells with OP9-DL4 cells, WT and $Bcl6^{-/-}$ DN4 cells sorted from these co-cultures generated similar frequencies of ISP and DP cells in the presence and absence of IL-7 (Fig. 6b), suggesting that *Bcl6* does not obviously regulate differentiation during β-selection. Similar to the experiment shown in Fig. 4c, IL-7 significantly increased the number of WT DN4 cells recovered after 2 days (Fig. 6c). Interestingly, *Bcl6* deficiency significantly increased recovery of DN4 cells in the absence of

IL-7 (Fig. 6c). Furthermore, the number of $Bcl6^{-/-}$ DN4 cells recovered from cultures without IL-7 was not significantly different from the number of WT DN4 cells recovered from cultures with IL-7, suggesting that repression of $Bcl6$ is a major mechanism by which IL-7 induces DN4 self-renewal. Nonetheless, IL-7 addition further augmented proliferation of $Bcl6^{-/-}$ DN4 cells, suggesting that $Bcl6$ deletion does not fully recapitulate the proliferation-inducing functions of IL-7.

IL-7 impact on ISP thymocytes

We also investigated ISP generation in the absence of IL-7 signaling *in vivo*. ISP numbers (defined as shown in Supplementary Fig. 4a) were 100-fold lower in $Il7r^{-/-}$ than $Il7r^{+/+}$ mice (Fig. 7a), in keeping with the reduced pools of all upstream progenitors (Fig. 2b). However, in striking contrast to $Il7r^{-/-}$ DN4 cells, $Il7r^{-/-}$ ISP were large CD71^{hi} CD98^{hi} cells, similar to WT ISP (Supplementary Fig. 4b). Expression of CD71 and CD98 in eDP and lDP also persisted in the absence of IL-7 signaling (Supplementary Fig. 4c). $Il7^{+/+}$ and $Il7^{-/-}$ ISP generated DP progeny *in vitro* with similar kinetics (Fig. 7b), suggesting that IL-7 deficiency does not impact the ISP-DP transition. Thus, although loss of IL-7 signaling impaired DN4 trophic responses and accelerated their differentiation, it did not impact these functions in ISP or DP cells. Nonetheless, $Il7r^{-/-}$ ISP generated *in vivo* (Fig. 7a) and *in vitro* (Supplementary Fig. 3a) abnormally expressed CD25, suggesting that in the absence of IL-7 signaling, most ISP seem to arise directly from CD25^{+} DN3b cells rather than from CD25^{−} DN4 cells.

To directly evaluate the DN3b–DP transition *in vivo*, we tracked differentiation of proliferating cells in $Il7r^{-/-}$ versus $Il7r^{+/+}$ mice at various times after BrdU injection. As expected, DN3a cells from both strains of mice were quiescent (mostly BrdU[−]) 2h after injection, but accumulated label from proliferating precursors over the next 24–48h (Fig. 7c). Thus, the absence of intrathymic IL-7 signaling did not impact DN3a generation from proliferating precursors but greatly decreased DN3a survival (Fig. 2). In contrast to quiescent DN3a cells, 65–75% of WT DN3b, DN4 and ISP cells were BrdU[+] after 2h, confirming that each subset is rapidly cycling (Fig. 7d). Labeled DN3b cells decreased after 24h, consistent with derivation from quiescent DN3a precursors, whereas DN4 and ISP cells were highly labeled, consistent with their derivation from cycling DN3b and DN4 precursors, respectively. As shown earlier (Fig. 4), only ∼10% of $Il7r^{-/-}$ DN4 cells were BrdU[+] 2h after injection. However, 70–90% of $Il7r^{-/-}$ DN3b cells were BrdU[+] (Fig. 7d), suggesting that most DN4 cells are derived from quiescent DN3a cells rather than cycling DN3b cells in $Il7r$ mutant mice. Indeed, BrdU accumulated in $Il7r^{-/-}$ DN4 cells slowly over the next 2 days, similar to both WT and mutant DN3a cells. Furthermore, $Il7r^{-/-}$ ISP were highly labelled after 24h, suggesting that they are not derived from quiescent DN4 cells, but directly from cycling DN3b cells.

Impact of IL-7 on *Tcra* recombination

Primary *TCRA* recombination involving 3' Vα and 5' Jα gene segments normally initiates in eDP cells as they become quiescent lDP cells, with secondary recombination events that use more distal gene segments occurring exclusively in non-cycling lDP cells[10, 29]. Since DN4 cells generated in the absence of IL-7 were abnormally quiescent, we asked whether they

had undergone premature *Tcra* recombination. We sorted DN4, ISP and eDP and lDP thymocytes from *Il7*$^{-/-}$ versus *Il7*$^{+/+}$ mice and used qPCR to quantify primary *Tcra* rearrangements involving 3' *Vα17* (*Trav17*) and 5' *Jα61* (*Traj61*) and *Jα56* (*Traj56*) as well as secondary rearrangements involving more 5' *Vα12* (*Trav12*) and 3' *Jα42* (*Traj42*), *Jα30* (*Traj30*) and *Jα17* (*Traj17*) segments.

As expected, we detected very low amounts of primary and secondary *Tcra* rearrangements in cycling WT DN4, ISP and CD71$^+$ CD98$^+$ eDP cells, whereas we detected high levels of both primary and secondary rearrangements in post-mitotic CD71$^-$ CD98$^-$ lDP cells (Fig. 8a,b). In striking contrast, *Il7*$^{-/-}$ DN4 cells had abundant primary and secondary rearrangements that were comparable in frequency to those found in WT lDP cells. Thus, abnormally quiescent DN4 cells from IL-7-deficient mice undergo premature and extensive *Tcra* recombination. Nonetheless, *Il7*$^{-/-}$ ISP and eDP cells had very low levels of both primary and secondary *Tcra* rearrangements, similar to levels seen in WT ISP and eDP cells. Furthermore, we did not detect *Tcra* rearrangements in *Il7*$^{-/-}$ DN3b cells (data not shown). The sharp contrast in *Tcra* rearrangement status between quiescent DN4 relative to cycling ISP and eDP cells from *Il7*$^{-/-}$ mice provides further evidence that DN4 cells are not precursors of ISP and eDP cells in these mutant mice.

The extensive rearrangement of *Tcra* in *Il7*$^{-/-}$ DN4 cells suggested that they prematurely up-regulated *Rag1/2* expression. However, our gene expression profiling experiments showed that IL-7 treatment (for 3 h) did not acutely decrease *Rag1/2* expression in DN3b or DN4 thymocytes, in contrast to direct STAT5 targets such as *Cish* (Fig. 8c) and *Bcl6* (Fig. 6a). Thus, *Rag* genes do not appear to be direct transcriptional targets of IL-7 in DN thymocytes. Nonetheless, *Rag1* and *Rag2* mRNA levels were significantly higher in DN4 cells isolated from *Il7*$^{-/-}$ relative to WT mice (Fig. 8d), likely reflecting their accelerated differentiation in the absence of IL-7. Interestingly, Rag2 undergoes cyclin-A/cdk2-mediated proteolysis during S-phase to minimize the oncogenic potential of Rag-induced DNA breaks in cycling cells[30] . Since IL-7-deficient DN4 cells were abnormally quiescent, we also evaluated Rag2 protein abundance by immunoblotting (Fig. 8e). As expected, Rag2 expression was low in cycling DN3b and eDP cells but high in quiescent lDP cells from both WT and *Il7*$^{-/-}$ mice. In striking contrast, Rag2 was barely detectable in cycling DN4 cells from WT mice, but was readily detected in quiescent DN4 cells from *Il7*$^{-/-}$ mice, even though the low DN4 abundance in *Il7*$^{-/-}$ mice necessitated under-loading this lane. Notably, Rag2 expression was not elevated in cycling DN3b cells from *Il7*$^{-/-}$ mice, suggesting that loss of IL-7 signaling is not sufficient to increase Rag2 in cycling cells. Collectively, these data suggest that IL-7 deficiency promotes premature Rag1/2 re-expression and *Tcra* rearrangement by preventing cycling and accelerating differentiation of DN4 cells (summarized in Supplementary. Fig. 5).

DISCUSSION

Our study has demonstrated that the absence of intrathymic IL-7 signaling causes several striking abnormalities during β-selection that were not ameliorated by transgenic *BCL2*. During β-selection in WT mice, the canonical differentiation sequence is linear: DN3a–DN3b–DN4-ISP-eDP-lDP. In contrast, we provide *in vitro* and *in vivo* evidence that DP

cells arise via 2 abnormal pathways in IL-7 mutant mice. In one pathway, DN3a cells generate DN4 cells that prematurely up-regulate *Bcl6*, fail to self-renew and rapidly differentiate into lDP cells without obviously passing through the ISP stage. IL-7-deficient quiescent DN4 cells also prematurely re-express *Rag1* and *Rag2*, allowing premature primary and secondary *Tcra* recombination. However, there is also a "cycling" pathway, in which some DN3a cells generate cycling DN3b progeny that differentiate into DP cells via ISP intermediates that express CD25, and thus do not appear to transit through the DN4 stage. The abnormal retention of CD25 by proliferating post-β-selection cells in IL-7 mutant mice may suggest abnormal persistence of Notch signaling, since *Il2ra* is a direct Notch target in DN thymocytes[31]. Interestingly, IL-7 increased ISP frequency when added to WT DN3b and DN4 cells or to *Il7*^{−/−} DN3b cells. Since ISP cells do not express IL7R[18], IL-7 acts on DN3b and/or DN4 cells to enhance ISP generation and/or delay their differentiation into DP cells. Thus, IL-7 signaling in DN3 and DN4 cells may delay some aspects of differentiation during the DN3b–DP transition. Collectively these findings demonstrate that IL-7 signaling is required to maintain DN4 self-renewal, to enforce the canonical DN3a–DN3b–DN4-ISP-DP differentiation sequence, and to delay *Tcra* rearrangement until after proliferation ceases during thymocyte β-selection.

In agreement with a previous study[21], we found that IL7R expression was relatively higher in pre-TCR-signaled DN3b cells than in DN3a cells. However, in contrast to studies examining total DN3 and DN4 cells[19], we found that IL-7 robustly induces STAT5 phosphorylation and significantly increases *Bcl2* mRNA in icTCRβ[+] DN3b and DN4 thymocytes *in vitro*. Furthermore, we showed that IL-7 induces pSTAT5 and maintains mBcl-2 protein levels in DN3b and DN4 cells *in vivo*. Although a previous study concluded that IL-7 is needed to maintain survival but not proliferation of fetal DN4 thymocytes[21], we found that over-expression of hBcl-2 in *Il7r*^{−/−} mice did not restore DN3b, CD4, CD8 ISP or DP cells, despite significantly restoring the DN3a, CD4 and CD8 SP subsets. While we cannot rule out that IL-7 functions differ between fetal versus adult DN4 cells, our findings demonstrate that in addition to pre-TCR and Notch1, IL-7 signaling is maintained during β-selection *in vivo* and has important functions that cannot be replaced by *BCL2*.

Our study suggests that IL-7 signaling is required to prevent atrophy of DN4 cells and maintain their proliferation *in vivo*. Furthermore, IL-7 greatly enhanced Notch-dependent DN4 self-renewal *in vitro*. We identified several mechanisms underlying the trophic and pro-proliferative functions of IL-7 during β-selection. First, IL-7 maintained expression of CD71 and CD98 nutrient receptors in DN4 thymocytes, previously reported to be Notch-dependent *in vitro*[8, 23]. However, Notch activation sustains IL7R expression in some contexts[24, 25], so the Notch effect on CD71 and CD98 expression may be indirect. Indeed, treatment with IL-7 alone increased *Cd71* mRNA and protein expression in DN4 thymocytes, but was not sufficient to induce DN4 proliferation in the absence of Notch activation. Therefore, our data suggest that IL-7 collaborates with Notch1 to maintain nutrient receptor expression and proliferation in DN4 thymocytes. Second, IL-7 induces expression of a surprisingly complex array of cell growth regulators in DN thymocytes, including metabolic enzymes, translational regulators and nutrient transporters. Most genes were more potently induced in pre-selection DN3a cells, suggesting that the profound

impact of IL-7 during β-selection could be partly due to changes induced prior to pre-TCR expression. Nonetheless, a small group of genes were more potently induced in post-selection DN thymocytes, suggesting that they may be co-operatively regulated by pre-TCR plus IL-7 signaling. Finally, *Bcl6* deletion partially restored DN4 self-renewal in the absence of IL-7, revealing that repression of *Bcl6* is an important function of IL-7 during β-selection. Although *Bcl6* promotes self-renewal of pre-B cells by limiting p53-induced apoptosis[15], hBcl-2 over-expression did not restore DN4 cellularity in IL-7-deficient mice. Thus, *Bcl6* likely limits DN4 self-renewal by inhibiting proliferation, perhaps by repressing *Myc*[32], rather than by simply promoting survival. Overall, our data suggest that during β-selection, IL-7 co-operates with pre-TCR-Notch signaling to re-program metabolism and translation to meet the biosynthetic demands of clonal expansion by inducing large number of metabolic regulators and repressing *Bcl6*. This prominent role for IL-7 in regulating metabolism and proliferation of T cell precursors likely explains why this signaling pathway is frequently mutated in T cell leukemia[33].

Among cell growth regulators induced by IL-7, regulators of PI3K–mTOR signaling pathway are likely to be particularly important for β-selection. The importance of PI3K signaling in β-selection was first revealed by the observation that deletion of *Pten*, a lipid phosphatase that counteracts PI3K function, greatly restores the DP thymocyte pool in mice with mutations that compromise pre-TCR or IL7R signaling[34]. *Pi3kcd* is the isoform required for β-selection[35], and its expression was acutely enhanced by IL-7 in both pre- and post-β-selection thymocytes, suggesting a positive feedback loop. PI3K leads to AKT activation and mTOR signaling to increase nutrient uptake and metabolism during proliferation. However, serum and glucocorticoid-induced protein kinase (SGK), rather than AKT, may control cell growth and metabolism downstream of mTOR signaling[36]. Since *Sgk1* was more strongly induced by IL-7 in DN3b and DN4 cells than in DN3a cells, this kinase may have particularly important roles for inducing clonal expansion of pre-TCR$^+$ cells.

Although pre-TCR signaling is thought to activate the Eα enhancer as early as the DN4 stage[12, 37, 38], in IL-7-sufficient mice very little *Tcra* recombination occurs until the DP stage. However, *Il7*$^{-/-}$ DN4 cells had high levels of primary and secondary *Tcra* rearrangements, similar to levels in WT lDP cells, revealing that IL-7 signaling normally prevents *Tcra* rearrangement in DN4 thymocytes. Several possible mechanisms could underlie this role for IL-7. During B cell development, IL-7-induced STAT5 tetramers directly repress *Igk* transcription and rearrangement via an epigenetic mechanism[13,14]. However, *Eα* does not contain consensus STAT5 binding sites, although several low stringency motifs are present (data not shown). Furthermore, a mechanism invoking active IL-7-induced repression of *Tcra* rearrangement does not readily explain the differential abundance of *Tcra* rearrangements in *Il7*$^{-/-}$ DN4 and lDP relative to *Il7*$^{-/-}$ ISP and eDP cells.

During B cell development, pre-BCR and IL-7 signaling co-operate to down-regulate *Rag1/2* expression by inhibiting Foxo transcriptions factors, thus preventing V(D)J recombination during pre-BCR-induced clonal expansion[39, 40, 41]. In contrast, IL-7 did not induce acute changes in *Rag1/2* expression in post-β-selection thymocytes in our study.

Nonetheless, DN4 cells generated in IL-7-deficient mice had higher steady mRNA levels, likely reflecting their accelerated differentiation kinetics. We also documented that non-cycling DN4 thymocytes from IL-7-deficient mice expressed higher Rag2 protein than cycling DN4 cells from WT mice, consistent with decreased cyclin-A-cdk2-mediated proteolysis of Rag2[30]. Therefore, our data suggest that IL-7 indirectly inhibits *Tcra* rearrangement by promoting DN4 cell proliferation and Rag2 degradation rather than by directly repressing *Rag1/2* expression. Collectively, our study shows that thymocyte β-selection is orchestrated by a complex interplay between pre-TCR, Notch and IL7R signaling.

ONLINE METHODS

Mice

C57BL/6J (referred to as WT, $Il7r^{+/+}$ or $Il7^{+/+}$) and $Il7r^{-/-}$[42] mice were purchased (Jackson Laboratories, Bar Harbor, ME. $Il7^{-/-}$ mice[43] were kindly provided by Dr. Rachel Gerstein (University of Massachusetts, Worchester Campus). *BCL2* transgenic mice used to generate $Il7r^{-/-}$ mice to generate $Il7r^{-/-}$ *BCL2* mice were previously described[44]. $Bcl6^{+/-}$ mice[27] were kindly provided by Dr. Riccardo Dalla-Favera (University of Colombia, NY). Genotypes were determined by PCR amplification of tail DNA as described previously[44]. For all experiments, thymocytes were harvested from 4–6 week-old mice. All mice were bred in the specific pathogen-free facility of Toronto Centre for Phenogenomics (Toronto, Ontario, Canada) and procedures were approved by its Animal Care Committee, following guidelines from the Canadian Council on Animal Care.

Flow Cytometry

Thymocyte single-cell suspensions were stained with fluorochrome-conjugated antibodies and secondary reagents and immunofluorescence was analyzed on a FACSLSR-II (BD Biosciences, San Jose, CA) as previously described[23]. Data files were analyzed with FlowJo (Tree Star, Ashland, OR). Dead cells and debris were excluded based on staining with propidium iodide (unfixed cells) or Fixable Blue Viability dye (Invitrogen, Grand Island, NY), versus forward scatter profiles. Thymocytes were stained with a cocktail of APC-conjugated antibodies specific for lineage (Lin) markers (CD19, Gr1, CD11b, NK1.1, δγTCR and CD11c) together with antibodies recognizing CD3 (Alexa-700), CD4 (EF450), CD8 (APC-EF780), CD25 (PE-Cy7) and CD71 (FITC) and CD98 (PE). To distinguish DN2 from DN3 cells (Fig. 2) CD44 (PE) was used instead of CD98. After gating out Lin$^+$ cells, DN3a (CD25$^+$ CD71^{lo} CD98^{lo}, DN3b (CD25$^+$ CD71^{hi} CD98^{hi}) and DN4 ($Il7^{+/+}$: CD25$^-$ CD71^{hi} CD98^{hi}; $Il7^{-/-}$: CD25$^-$CD71$^{hi/lo}$ CD98$^{hi/lo}$) thymocytes were sorted using a FACS AriaII (BD Biosciences). Purity was >98% for all sorted populations. For detection of icTCRβ and mBcl-2 or hBcl-2, cells were stained with Fixable Blue Viability dye (Invitrogen, Grand Island, NY) for 30' at 4°C, followed by antibodies specific for Lin markers, CD3, CD4, CD8, CD25, CD71 and CD98 prior to fixing, permeabilizing (Cytofix/Cytoperm kit, BD biosciences) and staining with antibodies specific for TCRβ (H57–597), mBcl-2 (3F11) or hBcl-2 (6C8) according to manufacturer's protocols (BD Biosciences).

Fluorochrome or biotin-conjugated antibodies specific for the following murine markers were used: IL7R (A7R34), CD19 (ID3), CD3 (145-2C11), CD4 (RM4–5), CD8a (53–6.7), CD45.1 (A20), CD45.2 (104), CD25 (7D4), TCRβ (H57–597), CD11b (M1/70), Gr-1 (RB6–8C5), Ly76 (Ter119), NK1.1 (PK136), CD11c (HL3), CD24 (M1/69), CD44 (IM781), CD27 (LG.3A10), CD71 (C2), CD98 (RL388) and CD117 (2B8). Antibody-fluorochrome conjugates and Avidin second-stage reagents were purchased from Pharmingen–BD Biosciences (San Diego, CA) or eBiosciences (San Diego, CA), and used at predetermined optimal concentrations. Statistical significance for all population comparisons was calculated using unpaired two-tailed T-tests. FMO controls included all antibodies except the one displayed on the x-axis in each Figure.

To assess thymocyte proliferation *in vivo*, 4 to 6-week-old $Il7r^{-/-}$, $Il7r^{-/-}$ BCL2 mice and age-matched $Il7r^{+/+}$ mice were injected twice with 1 mg BrdU (intra-peritoneally), 1h apart. Thymocytes were isolated 2, 24 or 48h after the first injection. BrdU incorporation was assessed after Fixable Blue staining using the BrdU Flow Kit (BD Biosciences) as per manufacturer's instructions.

pSTAT5 Staining

For *ex vivo* experiments, thymocyte suspensions were prepared in serum-free, phenol-free RPMI (Wisent Inc.), stained with Fixable Blue for 30' at 37°C and immediately fixed using BD Cytofix buffer, and then permeabilized using Phosphoflow BD Perm III buffer prior to staining with anti-pSTAT5(Y694) conjugated to Alexa647 and other antibodies. For detection of pSTAT5 after *in vitro* IL-7 stimulation, WT thymocytes were cultured with media or 10 ng/ml mIL-7 for 20', stained with Fixable Blue for 30' at 37°C, then fixed and permeablized as described above prior to staining with anti-pSTAT5(Y694).

Cell culture

Sorted thymocytes were seeded into 24-well plates containing 1 ml Iscove's media supplemented with 20% FBS, penicillin (100 U/ml), streptomycin (100 μg/ml) and IL7 (10 ng/ml), and were incubated at 37° C in a humidified atmosphere with 5% CO2 for the amount of time indicated in each Figure legend. To assess thymocyte proliferation *in vitro*, WT DN4 thymocytes were sorted and labeled with CFSE as described[23] prior to culture (5,000/well) in media alone or with 10 ng/ml of IL7 without stromal cells, or on 80% confluent monolayers of OP9-DL4 cells together with increasing doses of IL7: 0, 0.05, 0.5 and 5 ng/ml. After 15–40h (no stroma) or 48h (OP9-DL4), cells were stained with propidium iodide, followed by antibodies specific for CD4 and CD8, and CFSE levels and viable cell numbers were assessed by flow cytometry.

To assess the impact of *Bcl6* deletion effect on DN4 survival *in vitro*, Ter119⁻ CD19⁻ Gr1⁻ CD117⁺ cells from $Bcl6^{-/-}$ and $Bcl6^{+/+}$ fetal liver (15.5 dpc) were sorted and co-cultured (1,000/well) with OP9-DL4 cells and IL7 and Flt3 ligand as described[23], to induce their differentiation into T-lineage precursors. After 9 days, DN4 cells (Lin⁻ CD45.2⁺ CD4⁻ CD8⁻ CD44⁻ CD25⁻ CD27^hi) were sorted and re-cultured (3,000/well) on OP9-DL4 cells in media alone or with IL7 (10 ng/ml). After 2 days, CD4 vs CD8 expression and recovery of viable icTCRβ⁺ DN cells was quantified using flow cytometry.

Gene expression profiling

DN3a, DN3b and DN4 thymocytes were sorted from *Il7r*^{+/+} mice (4 independent sorts), rested for 1h at 37° C in a humidified atmosphere with 5% CO_2, and then left untreated or stimulated with IL-7 (10 ng/ml, Stem Cell Technologies) for 3h before isolating total cellular RNA using the RNeasy isolation kit (Qiagen). Quality control and quantitation was done on a Bioanalyzer 2100 (Agilent). Genome-wide expression profiling was carried out using Illumina mouse Ref8 v2 beadchips according to standard protocols at The Centre for Applied Genomics (TCAG, www.tcag.ca) core facility at the Hospital for Sick Children. Data processing and other statistical analyses were performed using R Bio-conductor 2.13.0. Raw signals from 25697 probes were pre-processed to perform background subtraction, quantile normalization and log2 transformation before using moderated *t*-tests within Bioconductor package Limma (Linear Models for Microarray Data). Empirical Bayes smoothing was applied to the standard errors. Paired *t*-tests were used to identify IL-7-induced changes in gene expression in each subset and the false discovery rate (FDR) was estimated using the Benjamini-Hochberg method to correct for multiple testing. Pearson correlations showed that technical replicates showed very high correlations between chips. For genes that were represented by multiple probesets on the array, we selected the ones with the highest ANOVA F-statistics (lowest FDR-adjusted *q*-value).

Gene Set Enrichment Analysis

Gene lists were ranked using the Limma moderated t-statistic, a value that reflects the magnitude of differential expression (based on mean expression value) as well as the variance of that gene's expression within each group. Parameters were set to 2000 gene-set permutations and gene-set sizes between 15 and 500 (www.broadinstitute.org). Gene-sets were obtained from KEGG, MsigDB-c2, NCI, Biocarta, IOB, Netpath, HumanCyc, Reactome and the Gene Ontology (GO) databases. Enrichment maps depicting relationships between significantly enriched gene-sets (nominal *p*<0.01, overlap coefficient=0.5) were generated using the Enrichment Plugin module (v1.2) of Cytoscape 2.8.1[45].

qRT-PCR

mRNA from sorted thymocytes was isolated with the RNeasy Plus Micro kit (Qiagen) and reverse-transcribed using the High Capacity cDNA Reverse Transcription Kit (Life Technologies). The abundance of *Cd45*, *Bcl6, Rag1* and *Rag2* cDNA in each sample was determined with Power SYBR Green (Life Technologies). Primers used were: *CD45* forward, 5'-AAGTCTCTACGCAAAGCACGG-3', *CD45* reverse, 5'-GATAGATGCTGGCGATGATGTC-3', *Bcl6* forward, 5'-CTGCAGATGGAGCATGTTGT-3', *Bcl6* reverse, 5'-GCCATTTCTGCTTCACTGG-3', *Rag1* forward, 5'- CTGTGGCATCGAGTGTTAACA-3', *Rag1* reverse, 5'-GCTCAGGGTAGACGGCAAG-3', *Rag2* forward, 5'-TGCCAAAATAAGAAAGAGTATTTCAC-3', *Rag2* reverse, 5'-GGGACATTTTTGATTGTGAATAGG-3'. The number of *Bcl6, Rag1* and *Rag2* templates was divided by the number of *Cd45* templates (mean of triplicate measurements) to obtain normalized expression values for each gene.

Tcra recombination

Genomic DNA was isolated from sorted thymocytes by standard procedures. Rearranged DNA was quantified by real-time PCR using a QuantiFast SYBR Green PCR kit (Qiagen). All PCR reactions were run in duplicate using the following amplification program: 95°C for 5m, followed by 45 cycles of 95°C for 10s and 62°C for 30s. Samples were normalized to signals for *B2m*. Primers used for *Tcra* rearrangement analysis were published elsewhere[46, 47, 48], except for *Traj30*: GGGAGAACATGAAGATGTGTCC.

Western blotting

Protein extracts were prepared from sorted thymocytes in modified radioimmuno-precipitation assay (RIPA) buffer [50 mM tris-Cl (pH 7.4), 1% NP-40, 0.25% sodium deoxycholate, 150 mM NaCl, 1 mM EDTA] with protease inhibitor (Roche) and separated by SDS–polyacrylamide gel electrophoresis. Proteins were transferred onto polyvinylidene difluoride membranes, which were cut into two parts at the level of the 50kDa marker before Western blotting overnight using standard techniques. The upper membrane was probed with rabbit anti-Rag2 antibody (EPRAGR239, Abcam) and the lower membrane was probed with rabbit anti-β-actin antibody (13E5, Cell Signaling). Both membranes were then probed with horseradish peroxidase–conjugated anti-rabbit IgG (7074, Cell Signaling) for 2 hours. Detection was performed with ECL reagents (GE Healthcare) and digitally measured using ChemiDoc MP (BioRad).

Statistical methods

Data were analyzed with a two-tailed Student T-test to compare means of 2 groups, and one-way ANOVA with Newman-Keuls post hoc T-test to compare means of 2 groups in experiments with 3 or more groups. *P* values of less than 0.05 were considered statistically significant. No randomization of mice or 'blinding' of researchers to sample identity was used during the analyses. Sample sizes were not predetermined on the basis of expected effect size, but rough estimations were made on the basis of pilot experiments and measurements. No data exclusion was applied.

Supplementary Material

Refer to Web version on PubMed Central for supplementary material.

Acknowledgements

REFERENCES

1. Yuan JS, Kousis PC, Suliman S, Visan I, Guidos CJ. Functions of notch signaling in the immune system: consensus and controversies. Annual review of immunology. 2010; 28:343–365.

2. Mazzucchelli R, Durum SK. Interleukin-7 receptor expression: intelligent design. Nature reviews Immunology. 2007; 7(2):144–154.

3. Akashi K, Kondo M, von Freeden-Jeffry U, Murray R, Weissman IL. Bcl-2 rescues T lymphopoiesis in interleukin-7 receptor-deficient mice. Cell. 1997; 89(7):1033–1041. [PubMed: 9215626]

4. Maraskovsky E, O'Reilly LA, Teepe M, Corcoran LM, Peschon JJ, Strasser A. Bcl-2 can rescue T lymphocyte development in interleukin-7 receptor-deficient mice but not in mutant rag-1–/– mice. Cell. 1997; 89(7):1011–1019. [PubMed: 9215624]

5. Khaled AR, Li WQ, Huang J, Fry TJ, Khaled AS, Mackall CL, et al. Bax deficiency partially corrects interleukin-7 receptor alpha deficiency. Immunity. 2002; 17(5):561–573. [PubMed: 12433363]

6. Pellegrini M, Bouillet P, Robati M, Belz GT, Davey GM, Strasser A. Loss of Bim increases T cell production and function in interleukin 7 receptor-deficient mice. The Journal of experimental medicine. 2004; 200(9):1189–1195. [PubMed: 15504823]

7. Guidos CJ. Synergy between the pre-T cell receptor and Notch: cementing the alphabeta lineage choice. The Journal of experimental medicine. 2006; 203(10):2233–2237. [PubMed: 17000868]

8. Kelly AP, Finlay DK, Hinton HJ, Clarke RG, Fiorini E, Radtke F, et al. Notch-induced T cell development requires phosphoinositide-dependent kinase 1. The EMBO journal. 2007; 26(14): 3441–3450. [PubMed: 17599070]

9. Yannoutsos N, Wilson P, Yu W, Chen HT, Nussenzweig A, Petrie H, et al. The role of recombination activating gene (RAG) reinduction in thymocyte development in vivo. The Journal of experimental medicine. 2001; 194(4):471–480. [PubMed: 11514603]

10. Seitan VC, Hao B, Tachibana-Konwalski K, Lavagnolli T, Mira-Bontenbal H, Brown KE, et al. A role for cohesin in T-cell-receptor rearrangement and thymocyte differentiation. Nature. 2011; 476(7361):467–471. [PubMed: 21832993]

11. Shih HY, Hao B, Krangel MS. Orchestrating T-cell receptor alpha gene assembly through changes in chromatin structure and organization. Immunologic research. 2011; 49(1–3):192–201. [PubMed: 21128009]

12. del Blanco B, Garcia-Mariscal A, Wiest DL, Hernandez-Munain C. Tcra enhancer activation by inducible transcription factors downstream of pre-TCR signaling. Journal of immunology. 2012; 188(7):3278–3293.

13. Malin S, McManus S, Cobaleda C, Novatchkova M, Delogu A, Bouillet P, et al. Role of STAT5 in controlling cell survival and immunoglobulin gene recombination during pro-B cell development. Nature immunology. 2010; 11(2):171–179. [PubMed: 19946273]

14. Mandal M, Powers SE, Maienschein-Cline M, Bartom ET, Hamel KM, Kee BL, et al. Epigenetic repression of the Igk locus by STAT5-mediated recruitment of the histone methyltransferase Ezh2. Nature immunology. 2011; 12(12):1212–1220. [PubMed: 22037603]

15. Duy C, Yu JJ, Nahar R, Swaminathan S, Kweon SM, Polo JM, et al. BCL6 is critical for the development of a diverse primary B cell repertoire. The Journal of experimental medicine. 2010; 207(6):1209–1221. [PubMed: 20498019]

16. Walker SR, Nelson EA, Frank DA. STAT5 represses BCL6 expression by binding to a regulatory region frequently mutated in lymphomas. Oncogene. 2007; 26(2):224–233. [PubMed: 16819511]

17. Basso K, Dalla-Favera R. BCL6: master regulator of the germinal center reaction and key oncogene in B cell lymphomagenesis. Advances in immunology. 2010; 105:193–210. [PubMed: 20510734]

18. Yu Q, Erman B, Park JH, Feigenbaum L, Singer A. IL-7 receptor signals inhibit expression of transcription factors TCF-1, LEF-1, and RORgammat: impact on thymocyte development. The Journal of experimental medicine. 2004; 200(6):797–803. [PubMed: 15365098]

19. Van De Wiele CJ, Marino JH, Murray BW, Vo SS, Whetsell ME, Teague TK. Thymocytes between the beta-selection and positive selection checkpoints are nonresponsive to IL-7 as assessed by STAT-5 phosphorylation. Journal of immunology. 2004; 172(7):4235–4244.

20. Balciunaite G, Ceredig R, Fehling HJ, Zuniga-Pflucker JC, Rolink AG. The role of Notch and IL-7 signaling in early thymocyte proliferation and differentiation. European journal of immunology. 2005; 35(4):1292–1300. [PubMed: 15770699]

21. Trigueros C, Hozumi K, Silva-Santos B, Bruno L, Hayday AC, Owen MJ, et al. Pre-TCR signaling regulates IL-7 receptor alpha expression promoting thymocyte survival at the transition from the double-negative to double-positive stage. European journal of immunology. 2003; 33(7):1968–1977. [PubMed: 12884863]

22. Sinclair LV, Rolf J, Emslie E, Shi YB, Taylor PM, Cantrell DA. Control of amino-acid transport by antigen receptors coordinates the metabolic reprogramming essential for T cell differentiation. Nature immunology. 2013; 14(5):500–508. [PubMed: 23525088]

23. Yuan JS, Tan JB, Visan I, Matei IR, Urbanellis P, Xu K, et al. Lunatic Fringe prolongs Delta/Notch-induced self-renewal of committed alphabeta T-cell progenitors. Blood. 2011; 117(4):1184–1195. [PubMed: 21097675]

24. Magri M, Yatim A, Benne C, Balbo M, Henry A, Serraf A, et al. Notch ligands potentiate IL-7-driven proliferation and survival of human thymocyte precursors. European journal of immunology. 2009; 39(5):1231–1240. [PubMed: 19350552]

25. Gonzalez-Garcia S, Garcia-Peydro M, Martin-Gayo E, Ballestar E, Esteller M, Bornstein R, et al. CSL-MAML-dependent Notch1 signaling controls T lineage-specific IL-7R{alpha} gene expression in early human thymopoiesis and leukemia. The Journal of experimental medicine. 2009; 206(4):779–791. [PubMed: 19349467]

26. Petrie HT, Hugo P, Scollay R, Shortman K. Lineage relationships and developmental kinetics of immature thymocytes: CD3, CD4, and CD8 acquisition in vivo and in vitro. The Journal of experimental medicine. 1990; 172(6):1583–1588. [PubMed: 2147945]

27. Ye BH, Cattoretti G, Shen Q, Zhang J, Hawe N, de Waard R, et al. The BCL-6 proto-oncogene controls germinal-centre formation and Th2-type inflammation. Nature genetics. 1997; 16(2):161–170. [PubMed: 9171827]

28. Dent AL, Shaffer AL, Yu X, Allman D, Staudt LM. Control of inflammation, cytokine expression, and germinal center formation by BCL-6. Science. 1997; 276(5312):589–592. [PubMed: 9110977]

29. Krangel MS. Mechanics of T cell receptor gene rearrangement. Current opinion in immunology. 2009; 21(2):133–139. [PubMed: 19362456]

30. Zhang L, Reynolds TL, Shan X, Desiderio S. Coupling of V(D)J recombination to the cell cycle suppresses genomic instability and lymphoid tumorigenesis. Immunity. 2011; 34(2):163–174. [PubMed: 21349429]

31. Maillard I, Tu L, Sambandam A, Yashiro-Ohtani Y, Millholland J, Keeshan K, et al. The requirement for Notch signaling at the beta-selection checkpoint in vivo is absolute and independent of the pre-T cell receptor. The Journal of experimental medicine. 2006; 203(10):2239–2245. [PubMed: 16966428]

32. Nahar R, Ramezani-Rad P, Mossner M, Duy C, Cerchietti L, Geng H, et al. Pre-B cell receptor-mediated activation of BCL6 induces pre-B cell quiescence through transcriptional repression of MYC. Blood. 2011; 118(15):4174–4178. [PubMed: 21856866]

33. Inaba H, Greaves M, Mullighan CG. Acute lymphoblastic leukaemia. Lancet. 2013

34. Hagenbeek TJ, Naspetti M, Malergue F, Garcon F, Nunes JA, Cleutjens KB, et al. The loss of PTEN allows TCR alphabeta lineage thymocytes to bypass IL-7 and Pre-TCR-mediated signaling. The Journal of experimental medicine. 2004; 200(7):883–894. [PubMed: 15452180]

35. Janas ML, Varano G, Gudmundsson K, Noda M, Nagasawa T, Turner M. Thymic development beyond beta-selection requires phosphatidylinositol 3-kinase activation by CXCR4. The Journal of experimental medicine. 2010; 207(1):247–261. [PubMed: 20038597]

36. Pearce LR, Komander D, Alessi DR. The nuts and bolts of AGC protein kinases. Nature reviews Molecular cell biology. 2010; 11(1):9–22. [PubMed: 20027184]

37. Hernandez-Munain C, Roberts JL, Krangel MS. Cooperation among multiple transcription factors is required for access to minimal T-cell receptor alpha-enhancer chromatin in vivo. Molecular and cellular biology. 1998; 18(6):3223–3233. [PubMed: 9584163]

38. Taghon T, Yui MA, Pant R, Diamond RA, Rothenberg EV. Developmental and molecular characterization of emerging beta- and gammadelta-selected pre-T cells in the adult mouse thymus. Immunity. 2006; 24(1):53–64. [PubMed: 16413923]

39. Amin RH, Schlissel MS. Foxo1 directly regulates the transcription of recombination-activating genes during B cell development. Nature immunology. 2008; 9(6):613–622. [PubMed: 18469817]

40. Johnson K, Hashimshony T, Sawai CM, Pongubala JM, Skok JA, Aifantis I, et al. Regulation of immunoglobulin light-chain recombination by the transcription factor IRF-4 and the attenuation of interleukin-7 signaling. Immunity. 2008; 28(3):335–345. [PubMed: 18280186]

41. Timblin GA, Schlissel MS. Ebf1 and c-Myb repress rag transcription downstream of Stat5 during early B cell development. Journal of immunology. 2013; 191(9):4676–4687.

42. Peschon JJ, Morrissey PJ, Grabstein KH, Ramsdell FJ, Maraskovsky E, Gliniak BC, et al. Early lymphocyte expansion is severely impaired in interleukin 7 receptor-deficient mice. The Journal of experimental medicine. 1994; 180(5):1955–1960. [PubMed: 7964471]

43. von Freeden-Jeffry U, Vieira P, Lucian LA, McNeil T, Burdach SE, Murray R. Lymphopenia in interleukin (IL)-7 gene-deleted mice identifies IL-7 as a nonredundant cytokine. The Journal of experimental medicine. 1995; 181(4):1519–1526. [PubMed: 7699333]

44. Matei IR, Gladdy RA, Nutter LM, Canty A, Guidos CJ, Danska JS. ATM deficiency disrupts Tcra locus integrity and the maturation of CD4+CD8+ thymocytes. Blood. 2007; 109(5):1887–1896. [PubMed: 17077325]

45. Smoot ME, Ono K, Ruscheinski J, Wang PL, Ideker T. Cytoscape 2.8: new features for data integration and network visualization. Bioinformatics. 2011; 27(3):431–432. [PubMed: 21149340]

46. Abarrategui I, Krangel MS. Regulation of T cell receptor-alpha gene recombination by transcription. Nature immunology. 2006; 7(10):1109–1115. [PubMed: 16936730]

47. Shih HY, Verma-Gaur J, Torkamani A, Feeney AJ, Galjart N, Krangel MS. Tcra gene recombination is supported by a Tcra enhancer- and CTCF-dependent chromatin hub. Proceedings of the National Academy of Sciences of the United States of America. 2012; 109(50):E3493–3502. [PubMed: 23169622]

48. Vacchio MS, Olaru A, Livak F, Hodes RJ. ATM deficiency impairs thymocyte maturation because of defective resolution of T cell receptor alpha locus coding end breaks. Proceedings of the National Academy of Sciences of the United States of America. 2007; 104(15):6323–6328. [PubMed: 17405860]
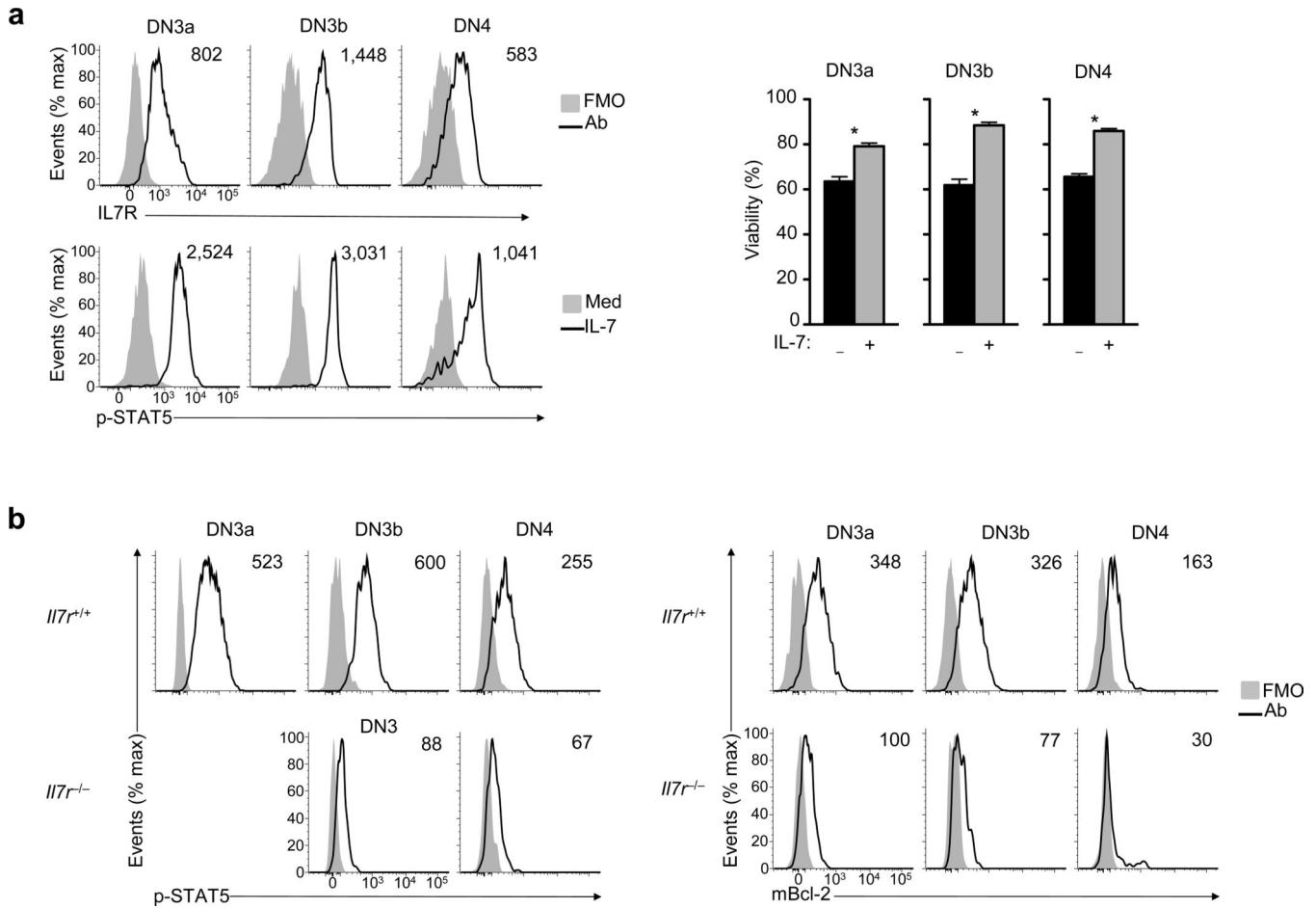
Figure 1.
Expression and function of IL-7R in pre- and post-β-selection thymocytes. (**a**) Flow
cytometry of DN3a (CD25$^+$icTCRβ$^-$), DN3b (CD25$^+$icTCRβ$^+$) and DN4 (CD25$^-$icTCRβ$^+$)
thymocytes from wild-type mice (gating strategy, Supplementary Fig. 1) and stained with
antibody to IL-7R (Anti-IL-7R), plotted with the fluorescence-minus-one background
control (top left), or cultured for 20' with (+) or without (−) IL-7 and stained with antibody
to phosphorylated STAT5 (p-STAT5) (bottom left); right, viability of cells cultured for
10-24 h with or without IL-7, analyzed by staining with propidium iodide and flow
cytometry. *P _0.0001 (unpaired two-tailed Student's t-test). (**b**) Flow cytometry of
DN3a, DN3b and DN4 *Il7r*$^{+/+}$ or *Il7r*$^{-/-}$ thymocytes that were immediately fixed,
permeabilized and stained with antibody to p-STAT5 (left), or stained with antibody to
mouse Bcl-2 (mBcl-2), plotted with background control as in a (right). Due to limited
cellularity, p-STAT5 was analyzed in total DN3 cells from *Il7r*$^{-/-}$ mice. Numbers in plots
(a, top left, and b) indicate normalized median fluorescence intensity of each marker,
calculated by subtraction of the median fluorescence intensity of the fluorescence-minus-one
control from that of fully stained cells. Numbers in a (bottom left) indicate normalized
median fluorescence intensity p-STAT5 calculated by subtracting the median fluorescence
intensity of cells cultured without IL-7 from that of cells cultured with IL-7. Flow cytometry
histograms are are representative of three independent experiments with similar results.

Viability graphs in a, right, show mean and s.d. of two biological replicates with two technical replicates per group in a, right.
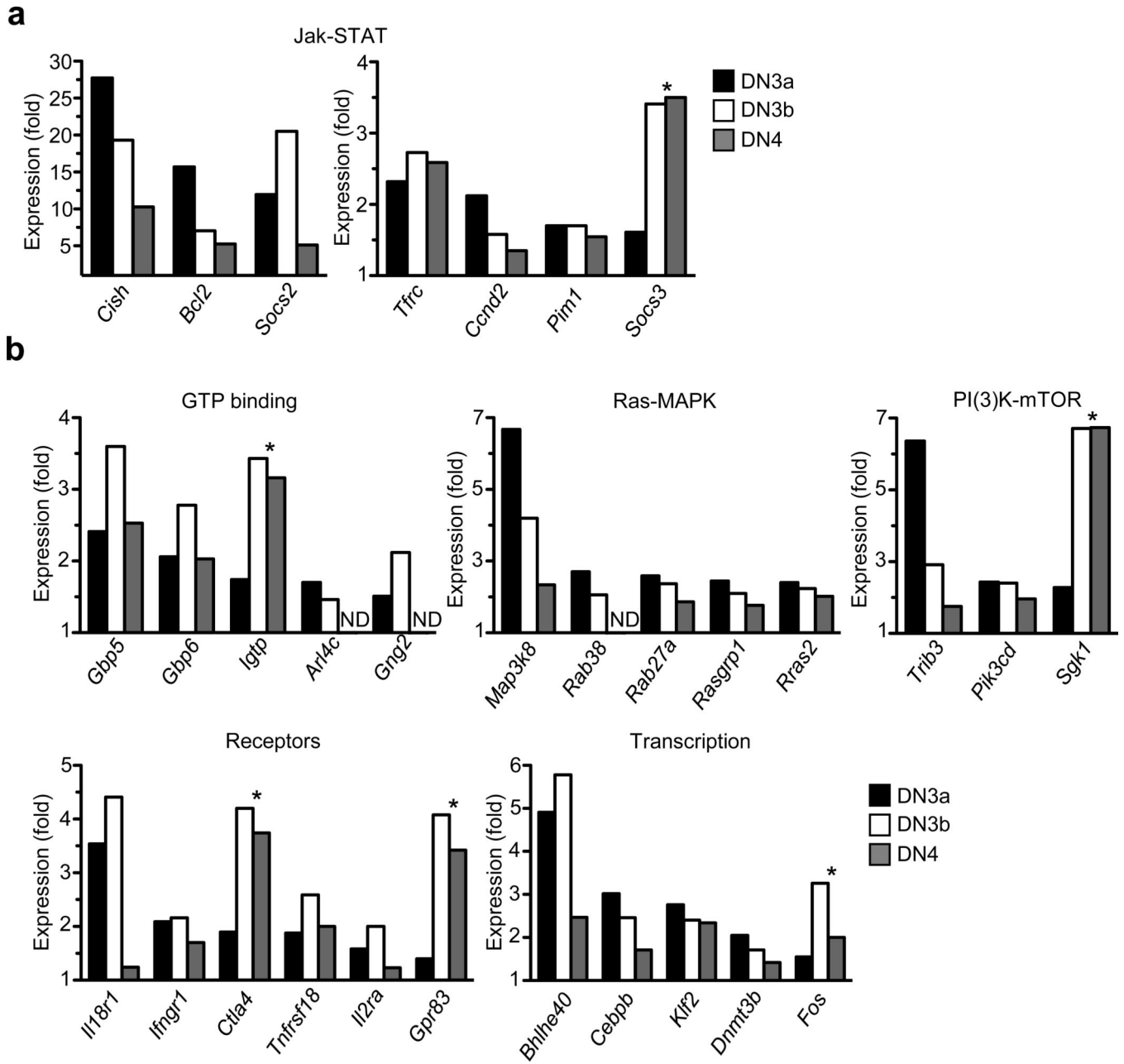
Figure 2.
hBcl-2 fails to compensate for loss of IL-7 signaling during β-selection. Thymocytes were counted and analyzed by flow cytomtery to calculate the frequency and total number of cells in each subset. (**a**) hBcl-2 expression (open) versus FMO control (shaded) in DN2, DN3, and DN4 thymocytes (gated as shown in Supplementary Fig. 1a, c) as well as DP, CD4 and CD8 subsets from $Il7r^{-/-}$ $BCL2$ mice. Numbers shown in the top right corner of each histogram depict normalized median fluorescence intensity (MFI) of hBcl-2 calculated by subtracting the MFI of the FMO from that of fully stained cells. Similar results were obtained in 3 individual experiments. (**b**) Bar graphs show the mean (+/− SD) number of cells in each subset for each strain: $Il7r^{+/+}$ (n=4), $Il7r^{-/-}$ (n=9) and $Il7r^{-/-}$ $BCL2$ (n=9). The

significance of differences between genotypes was assessed using Student's *t*-test as described for Fig. 1: *P<0.0001.

a

b
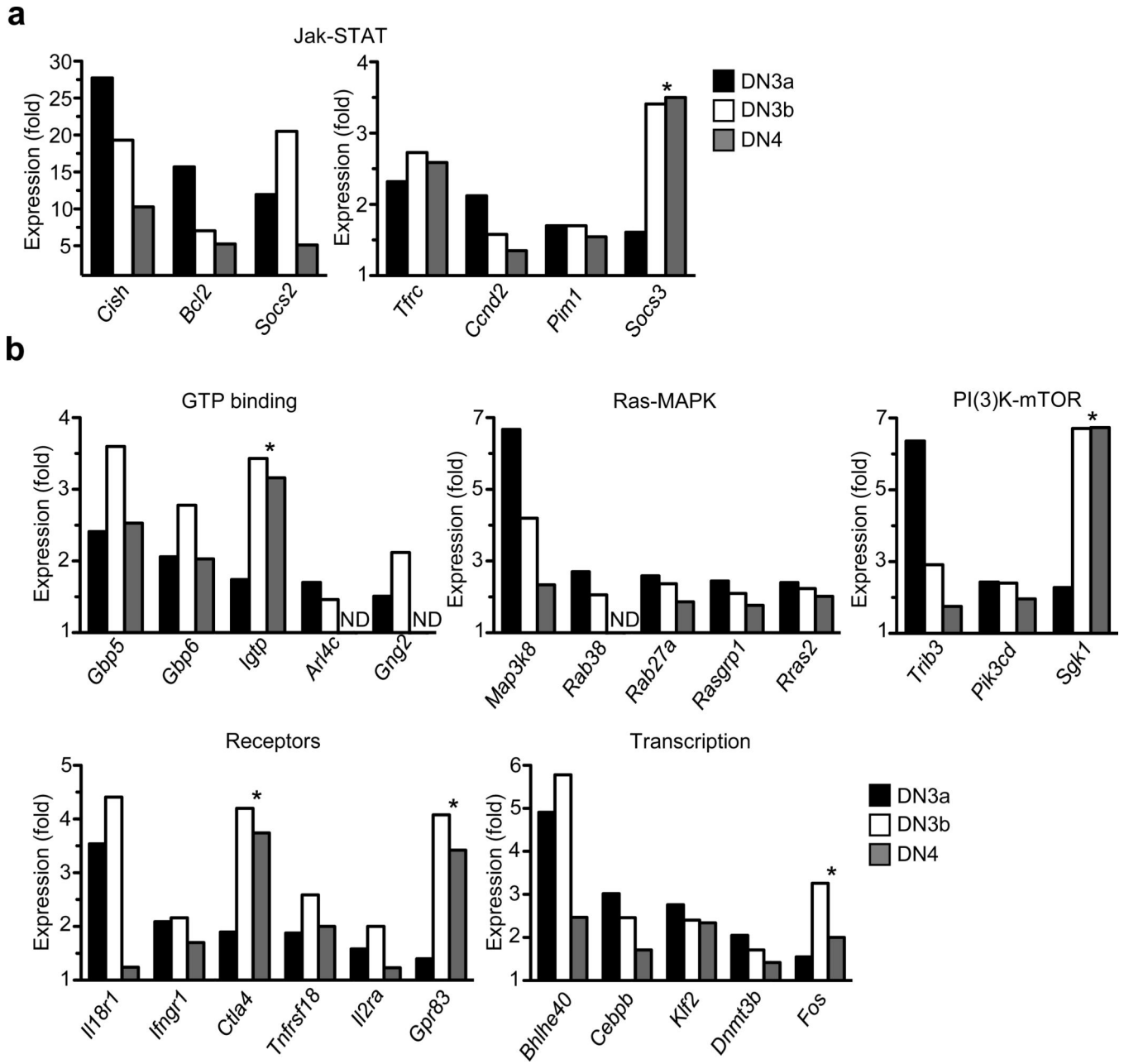
Figure 3.
Transcriptional response to IL-7 in DN3a, DN3b and DN4 thymocytes. Sorted subsets (4 biological replicates) were cultured with IL-7 (10 ng/ml) or media for 3h prior to isolating RNA and performing Illumina Ref8v2 gene expression profiling. After pre-processing, a paired empirical Bayes moderated *t*-test with Benjamin-Hochberg correction for multiple testing was conducted using Limma to select probe-sets significantly altered by IL-7 in each subset (FDR *q*<0.05), which were then collapsed into non-redundant gene lists. (**a,b**) Bar graphs depict the fold-change (FC) ratio (IL-7-stimulated/unstimulated) of normalized expression values for function-based groups of genes. Asterisks highlight genes more robustly induced by IL-7 in post-selection DN3b and DN4 relative to pre-selection DN3a

cells. FC ratios and FDR-adjusted q-values for each gene are indicated in Supplementary Table 2. ND: not detected.
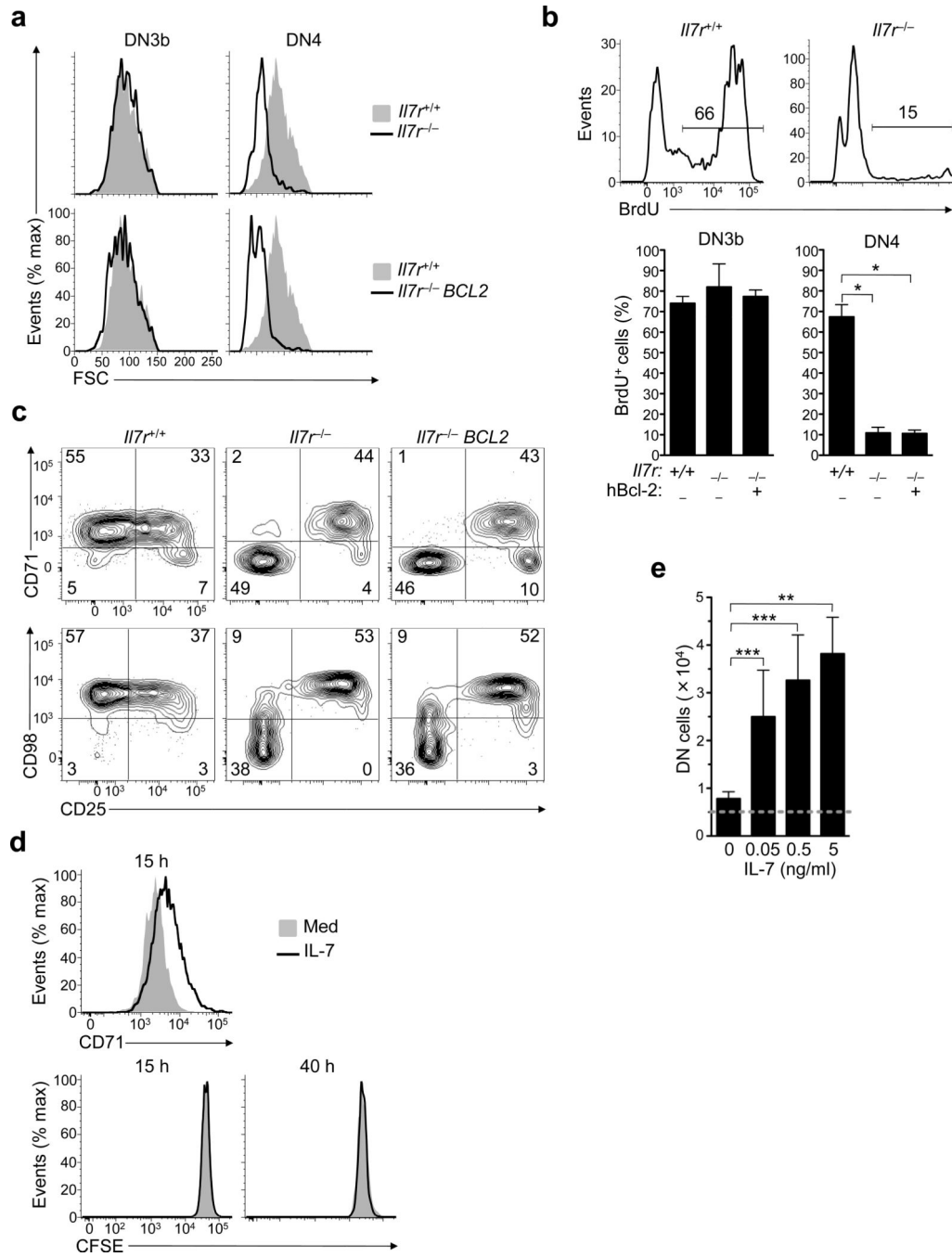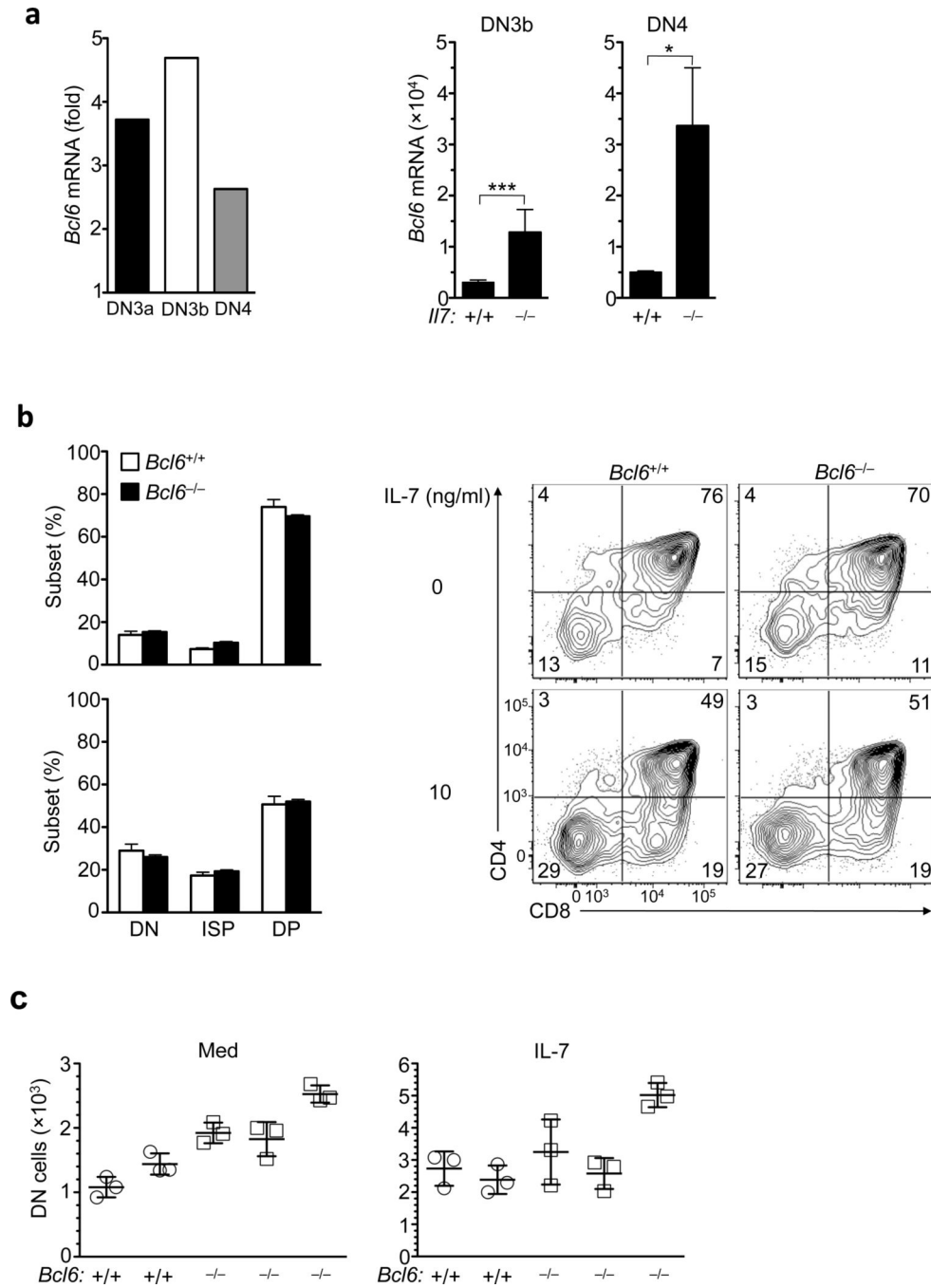
Figure 4.
IL-7 signaling promotes DN4 growth and proliferation *in vivo*. (**a**) Flow cytometric analysis of forward scatter (FSC), an indicator of cell size and metabolism, of each subset identified as described in Supplementary Fig. 1.: *Il7r*^+/+^ (shaded) versus *Il7r*^−/−^ (open) (Top). *Il7r*^+/+^ (shaded) versus *Il7r*^−/−^ *BCL2* (open) (Bottom). (**b**) Flow cytometric quantification of BrdU incorporation in DN4 cells (Top) from *Il7r*^+/+^ and *Il7r*^−/−^ mice, assessed 2h after the first BrdU injection and identified as shown in Supplementary Fig. 1. Bar graphs show % BrdU^+^ cells (mean +/− SD) in each subset from *Il7r*^+/+^ *Il7r*^−/−^ and *Il7r*^−/−^ *BCL2* mice (Bottom) (3

biological replicates/group). (**c**) Flow cytometric analysis of CD71 (Top) or CD98 (Bottom) vs CD25 expression, shown as 5% probability contour plots gated on DN CD3 Lin icTCRβ$^+$ thymocytes (**d**) Histograms show flow cytometric quantification of CD71 expression (Top) or CFSE (Bottom) after WT DN4 thymocytes were cultured in Med (shaded) or IL-7 (open) for 15 or 40h. (**e**) WT DN4 thymocytes (5×10^3/well, indicated by dotted horizontal line) were cultured with OP9-DL4 cells and media containing the indicated IL-7 concentrations for 48h. Bar graphs show the mean (+/− SD) number of DN cells recovered (3 technical replicates/group). The significance of differences between groups was assessed in (**b**) and (**e**) using one-way ANOVA with Newman-Keuls post hoc *t*-test. Similar results were obtained in 3 (**a, b, c, e**) or 2 independent experiments (**d**). *$P<0.001$, **$P<0.01$, ***$P<0.05$.

a

b

c
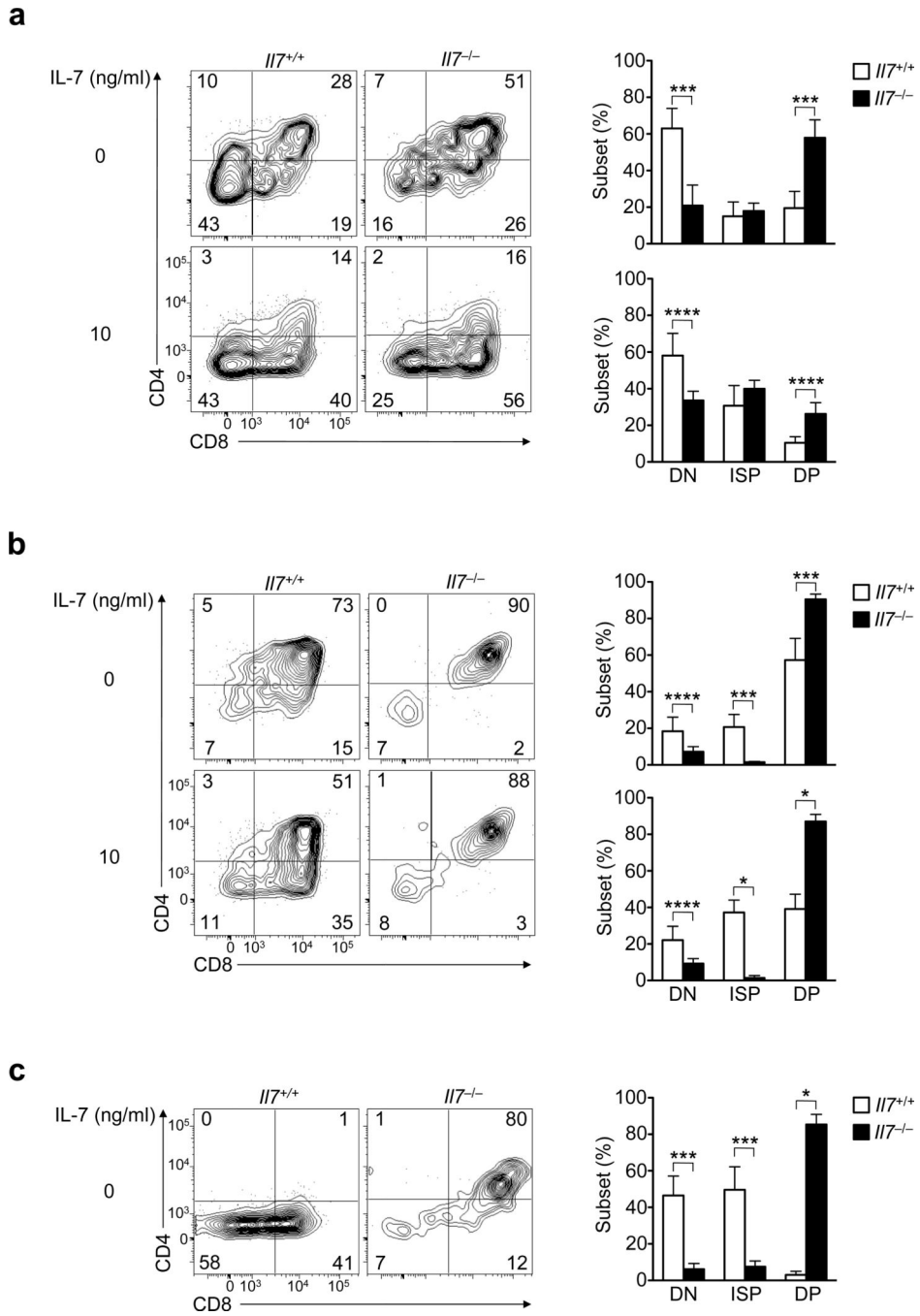
Figure 5.
IL-7 signaling delays DN3b and DN4 cell differentiation into DP thymocytes. DN3b or DN4 cells from $Il7^{+/+}$ and $Il7^{-/-}$ mice were cultured in the absence of stromal cells with or without IL-7 and analyzed by flow cytometry to assess the impact of IL-7 on their differentiation. (**a**) CD4 versus CD8 expression after DN3b cells from $Il7^{+/+}$ (white, 3 technical replicates/group) and $Il7^{-/-}$ (black, 4 technical replicates/group) mice were cultured for 15h without (Top) or with (Bottom) IL-7 (Left). Bar graphs show the % (mean +/− SD) of each subset after culture: DN (icTCRβ+ CD4 CD8, ISP (icTCRβ+ CD4 CD8+)

and DP (icTCRβ⁺ CD4⁺ CD8⁺) (Right). (**b,c**) DN4 cells from each genotype were cultured and analyzed by flow cytometry to assess the impact of IL-7 on their differentiation as described for (**a**). Bar graphs and contour plots show CD4 and CD8 expression on DN4 progeny after 15h without (Top) or with (Bottom) IL-7 (**b**, 4 technical replicates/genotype/group), or after 5h without IL-7 (**c**, 3 technical replicates/genotype/group). The significance of differences between means was calculated using Student's *t*-test as described for Fig. 1: *$P<0.0001$, **$P<0.001$, ***P 0.01, ****$P<0.05$. Similar results were obtained in at least 3 independent experiments (**a, b, c**).
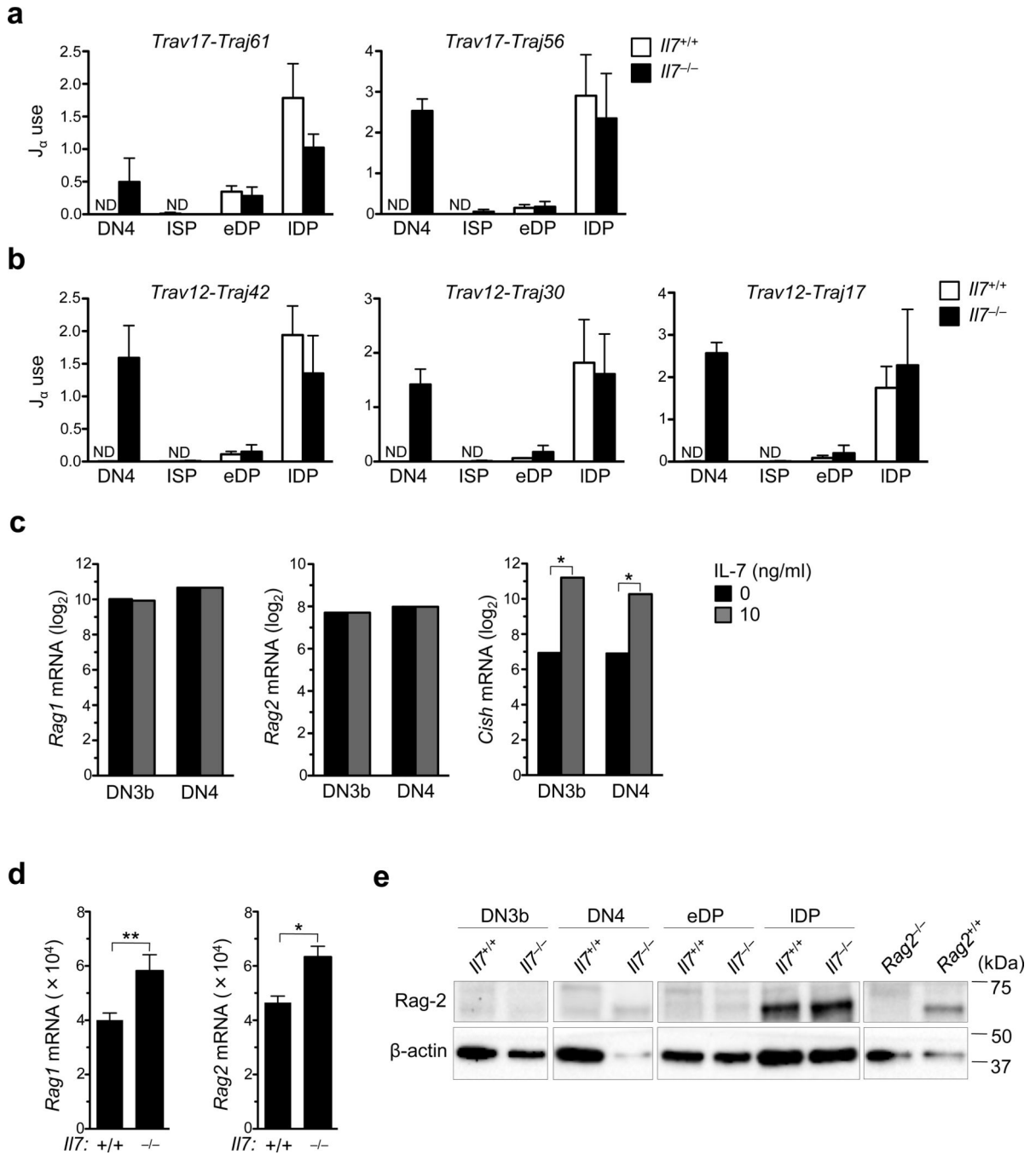
Figure 6.

Deletion of *Bcl6* improves the self-renewal of DN4 cells in the absence of IL-7. (**a**) *Bcl6* expression in DN3a, DN3b and DN4 wild-type cells cultured in IL-7, presented relative to its expression in their counterparts cultured in medium alone (as in Fig. 3; FDR-adjusted *q* values, Supplementary Table 2) (left), and quantitative RT–PCR analysis of *Bcl6* mRNA in DN3b and DN4 *Il7*^{+/+} and *Il7*^{−/−} thymocytes, normalized to results obtained for *Cd45* mRNA. (**b**) Quantification of cells in the DN, ISP and DP subsets (as in Fig. 5a) among the progeny of DN4 cells sorted from co-cultures of Bcl6+/+ and *Bcl6*^{−/−} fetal liver

hematopoietic progenitor cells cultured for 9 d with OP9-DL4 cells, then re-cultured (after sorting) for 48 h with or without IL-7 (left), and expression of CD4 versus CD8 by the sorted progeny of DN4 cells cultured with or without IL-7 (right), analyzed by flow cytometry (right). (**c**) Quantification of DN cells among the sorted DN4 cells in b cultured without or with IL-7. Each symbol represents an independent OP9 culture from two $Bcl6^{+/+}$ or three $Bcl6^{-/-}$ individual fetuses; small horizontal lines indicate the mean (±s.d.). *$P <$ 0.0001, **P 0.01 (Student's t-test (a)). Data are representative of two experiments with similar results (mean and s.d. of n = 3 technical replicates per group in a) or one experiment (b,c; mean and s.d. of n = 2 ($Bcl6^{+/+}$) or 3 ($^{Bcl6-/-}$) fetuses (three replicate cultures each)).
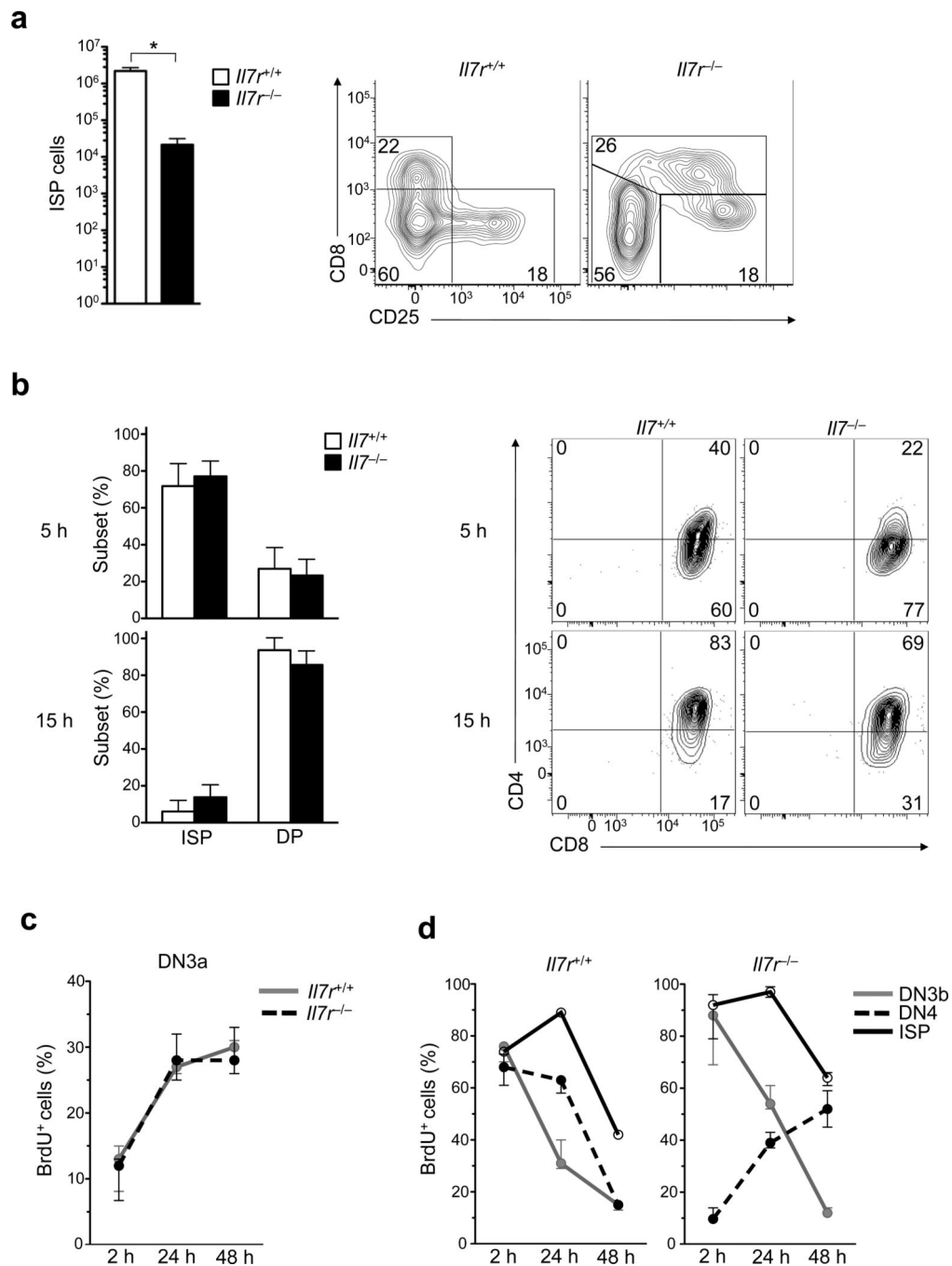
Figure 7.
Il7r^−/− DN4 thymocytes are not the precursors of ISP cell subset. (**a**) Left, thymocytes from
*Il7^+/+^* (*n*=4) and *Il7r^−/−^* (*n*=6) mice were counted and analyzed by flow cytometry to identify
ISP cells as CD3 CD24^+ cells within the Lin CD4 CD8^+ icTCRβ^+ subset (See
Supplementary Figure 4a). Right, contour plots show representative CD8 vs CD25
distribution gated on Lin CD3 CD4 icTCRβ^+ thymocytes. Gates identify ISP (CD25^−/+
CD8^+), DN4 (CD25 CD8^−/lo) and DN3b (CD25^+ CD8^−/lo) cells in each strain. (**b**) Sorted
ISP cells from each genotype were cultured for 5h (Top) or 15h (Bottom) without IL-7 (3

technical replicates/time point/genotype) and analyzed by flow cytometry as described for Fig. 5 to identify DP (CD4$^+$ CD8$^+$) and ISP (CD4 CD8$^+$) cells. (**c, d**) Thymocytes from *Il7r*$^{+/+}$ and *Il7r*$^{-/-}$ mice were harvested 2, 24 and 48h after BrdU injection (*n*=3 biological replicates/time-point/genotype) and analyzed by flow cytometry to measure % BrdU$^+$ (mean +/− SD) cells in DN3a (**c**), and DN3b (gray filled line), DN4 (black dashed line) and ISP (black filled line) subsets (**d**). Data for the 2h time-point were re-plotted here from Fig. 4b for comparison. Statistical significance in (**a**) was assessed using Student's *t*-test as described for Fig. 1: *P<0.0001. Similar results were obtained in 3 (**a, b**) or 2 (**c, d**) independent experiments.

Figure 8.
IL-7 signaling prevents premature recombination of *Tcra* locus in DN4 subset. (**a,b**) Genomic DNA from DN4, ISP, eDP (CD71^hi FSC^hi) and lDP (CD71^lo FSC^lo) thymocytes was analyzed by qPCR to measure *Vα*-to-*Jα* recombination using primers for *Trav17 (Vα17)* and proximal *Traj61 (Jα61)* and *Traj56 (Jα56)* segments (**a**), or primers for *Trav12* (which detect multiple, widely distributed *Trav12 (Vα12)* family members) and central *Traj42 (Jα42)* and *Traj30 (Jα30)* segments vs distal *Traj17 (Jα17)* segment (**b**). Bar graphs show relative *Jα* usage (mean ± SD) in each subset, normalized to levels detected in

unfractionated WT thymocytes (n=4, 2 biological replicates/subset/genotype and 2 technical replicate/sort). ND: not detected. (**c**) Bar graphs depict normalized expression values (Log$_2$ scale) for *Rag1, Rag2* and *Cish* from the Illumina mRNA expression profiling shown in Fig. 3. FDR-adjusted *q*-values for each comparison are indicated: *FDR *q*<0.0001. (**d**) qRT–PCR quantification of *Rag1* and *Rag2* mRNA in sorted *Il7*$^{+/+}$ and *Il7*$^{-/-}$ DN4 thymocytes (normalized to *CD45*, 3 technical replicates/group). The significance of differences between groups was assessed using Student's *t*-test as described for Fig. 1: *P<0.0001, **P<0.01. (**e**) Western blotting for Rag2 (top) and β-actin (bottom) protein in the indicated subsets from *Il7*$^{+/+}$ and *Il7*$^{-/-}$ thymi. Protein extracts from total *Rag2*$^{+/+}$ and *Rag2*$^{-/-}$ thymocytes were used as positive and negative controls, respectively. Similar results for each subset were obtained in 2 or more (**a, b**), 1 (**d**) and 3 (**e**) independent experiments.